

# HYDROGEN SAFETY: LAMINAR AND TURBULENT FLAME SPEED OF SPHERICAL FLAME IN A FAN-STIRRED CLOSED VESSEL

**J. Goulier, N. Chaumeix\***

Institut de Combustion, Aérothermique, Réactivité et Environnement, CNRS-ICARE  
1C, avenue de la recherche scientifique, 45071 Orléans cedex 2, France  
Jules.goulier@cns-orleans.fr; [chaumeix@cns-orleans.fr](mailto:chaumeix@cns-orleans.fr)

**N. Meynet, and A. Bentaïb**

Institut de Radioprotection et de Sûreté Nucléaire (IRSN)  
PSN-RES/SAG/B2EGR, BP 17, 92262 Fontenay-aux-Roses Cedex  
[nicolas.meynet@irsn.fr](mailto:nicolas.meynet@irsn.fr); ahmed.bentaib@irsn.fr

## ABSTRACT

The aim of this paper is to report new experimental results on the effect of turbulence on the propagation speed of hydrogen/air flames. To do so, a new experimental setup, spherical bomb, has been designed and built at CNRS-ICARE laboratory to investigate the effect of a given and well-characterized turbulence intensity on the increase of hydrogen/air flame speed. This new facility consists of a spherical vessel equipped (563 mm internal diameter) with 8 motors that can reach a rotation speed of 12 000 rpm. These engines are equipped with fans inside the bomb and when actuated can generate a turbulent flow inside the vessel prior to any ignition. The spherical bomb is equipped with 4 quartz windows (200 mm optical diameter) that allow the use of a PIV diagnostic in order to characterize the turbulence level inside the bomb. These experiments were performed for lean to stoichiometric hydrogen/air mixtures and for a rotation speed from 1000 to 5000 rpm. The PIV measurements showed that a homogeneous and isotropic turbulence is created with a fluctuation speed that can reach 4 m/s at 5000 rpm. Laminar and turbulent flame speeds of lean hydrogen-air mixtures at ambient temperature and pressure were measured using a high speed camera at 19 002 frames per second.

## KEYWORDS

Turbulent flame, Hydrogen Flame, Expanding flames, Turbulent intensity

## 1. INTRODUCTION

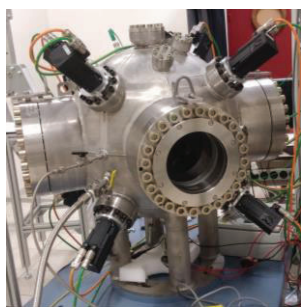
In case of a severe accident in a nuclear reactor with core meltdown, the interaction of the hot core with the cooling water can generate large amounts of hydrogen ( $H_2$ ). Hydrogen may be produced by the oxidation of metals present in the corium pool or in the basemat during the molten corium-concrete interaction phase. Since hydrogen/air mixtures exhibit a very low ignition energy, the presence of hot surfaces in the vicinity of the flammable mixture may lead to the ignition of a slow flame that can accelerate during its propagation leading to a fast flame which will be responsible for an overload threatening the nuclear reactor building. Hence, it is mandatory to understand the acceleration process and to be able to identify the phenomena that are responsible for this strong flame acceleration and from the

early beginning of the flame formation. Recent benchmarks [1, 2] have shown the importance of the turbulent flame models used in the CFD codes used worldwide in the assessment of the explosion risk in nuclear power plants. In fact, the lessons learnt from these benchmarks show that the computer codes are able to reproduce the maximum pressure generated by combustion. On the other hand, they do not well predict the flame propagation regimes as observed in the experiments and the rate of pressure increase. These exercises highlighted the need to measure the turbulence in the fresh gases and to characterize the transition from laminar flame to turbulent flame regime. These data are necessary for turbulent combustion models improvement and validation. Until now, this information is missing in the majority of the known experiments.

The aim of the present paper is to present new experimental results concerning laminar and turbulent flame speed of premixed hydrogen / air mixtures. The experiments are conducted in a closed spherical vessel in which a homogeneous and isotropic turbulence is generated using several fans. The first part of the paper will describe the experimental setup and the diagnostics and the second part of the paper will summarize the measured flame speeds and the temporal evolution of the combustion overpressure according to the fans rotations speeds (and hence turbulent intensity) for several conditions of molar percent of  $H_2$  in the mixture.

## 2. Experimental Setup

The laminar and turbulent combustion experiments have been performed in a spherical vessel with an inner diameter of 563 mm (total volume of 93.43 L), the wall thickness is 42 mm which allows the vessel to sustain a maximum pressure of 200 bar with an initial temperature ranging from ambient to 300°C (Fig.1-(a)). It is equipped with 4 quartz windows (200 mm optical diameter) which allow the implementation of optical diagnostics and 8 ports to mount the fans. Two tungsten electrodes are mounted along a diameter of the sphere, in the horizontal plane. They are linked to a high voltage discharge in order to create the electric spark necessary to ignite the mixture. The electric spark is used to trigger the recording equipment (camera and oscilloscopes) in order to synchronize the temporal flame growth with the evolution of the pressure inside the bomb. Indeed, the temporal behavior of the induced overpressure following the ignition is measured with two fast piezoelectric pressure transducer (Kistler 6001 and 601A models). They are mounted flush with inner wall of the vessel and located on opposite sides along a diameter of the bomb at +42° and -42° from the equatorial plan respectively.



(a)



(b)

Figure 1. Spherical bomb setup. (a) View of the spherical bomb with its equipment; (b) Image of the fan used in the turbulent experiments.

### 2.1. Flame visualization

The visualization of the flame was obtained using a Z-shape Schlieren apparatus (Fig.2-(a)). A white continuous lamp (300 W Xe Lot-Oriel lamp) is used to illuminate the flame via two lenses and two

concave spherical mirrors. A high speed camera (PHANTOM V1210), with an acquisition rate of 19002 frames per second, records the Schlieren images of the growing flame. The frame size was fixed to 768 x768 pixels<sup>2</sup>. An example of images acquired with the spherical bomb is given in Fig. 2-(b) and -(c).

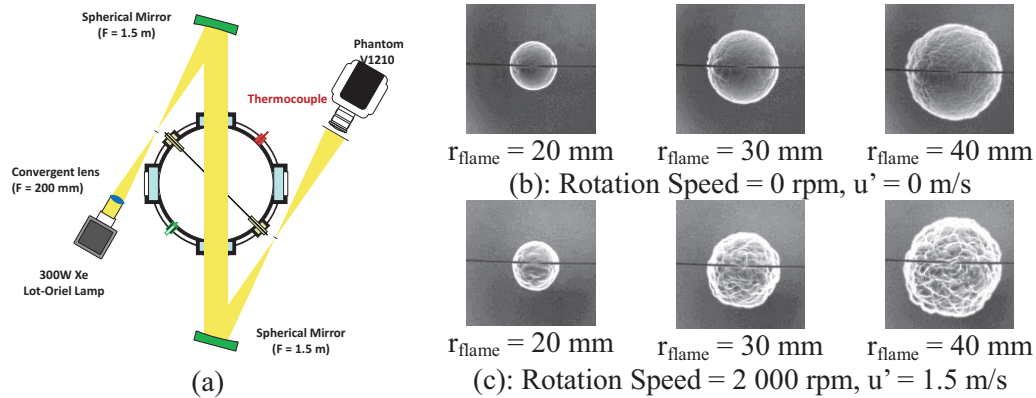


Figure 2. Optical arrangement for the Schlieren imaging and examples of images acquired for a mixture containing 24 %H<sub>2</sub> + 76 % Air initially at 1 atm and 296 K. (a): optical setup; (b): the mixture was initially at rest (turbulence intensity,  $u' = 0$ ); (c): the mixture was initially turbulent (turbulence intensity,  $u' = 1.5$  m/s).

## 2.2. Turbulence generation and characterization

The spherical bomb is equipped with 8 fans that are commercial impellers with 4 backward-curved blades with a diameter of 130 mm. They are propelled using 8 motors with a variable speed from 0 to 12 000 rpm. The flow, with these blades will be directed towards the vessel wall. A picture of the fan is given in Fig. 1-(b). The 8 fans are mounted symmetrically around the central circumference inside the vessel to generate the turbulence. They are located at the vertices of a fictitious cube inscribed within the spherical bomb. This symmetrical positioning induces a turbulent flow field characterized by several features: (i) a mean velocity close to zero, (ii) a homogeneous and isotropic turbulence within a central region inside the spherical chamber. In order to characterize the flow field inside the bomb when the fans are activated at a given speed, a series of experiments have been performed using a high resolution PIV system constituted of an Nd:YAG laser (Quantel Evergreen 200) delivering 2 pulses of 200 mJ at 532 nm, with a pulse width below 10 ns. The laser light was then expanded to a sheet with the lowest thickness, at the center of the bomb, equal to 0.5 mm with a semi-cylindrical lens (focal length=25 mm). With this arrangement it was possible to generate a laser sheet of 200 mm height. The seeding was created using Di-Ethyl-Hexyl-Sebacat (DEHS) oil with an in-house aerosol generator: the average diameter is around 0.3  $\mu\text{m}$  for these experiments. The camera used to image the laser light scattered by the seeding is TSI PowerView Plus 16MP which has a detector of 4920x3288 pixels<sup>2</sup> and the pixel size is 5.5  $\mu\text{m}^2$ . The obtained resolution was of 50  $\mu\text{m}/\text{pixel}$ . For each rotation speed of the fan, a minimum 800 couples of images are acquired in order to ensure of the validity of the statistical data processing. The time interval between the 2 pulses was chosen accordingly to the flow velocity to ensure that the displacement between 2 successive images is around 4 pixels in average. With this system, it was possible to measure the instantaneous velocity of the flow within a radius of 100 mm. From the averaging of the instantaneous velocity over more than 800 vector maps, it was possible to determine the average velocity components  $U(x,y)$  and  $V(x,y)$  in the two orthogonal directions  $(x,y)$ . Subtracting the average velocity from the instantaneous one led to the determination of the velocity fluctuation  $U_{\text{RMS}}$  and  $V_{\text{RMS}}$ . An example of the variation of the mean velocity and the fluctuation is given in Fig. 3 for two different rotation speeds of the fans. As one can see, both components of the mean velocity are very low and below 5 % of the corresponding fluctuation over a large radius in the spherical bomb (100 mm) which validate the

assumption that the mean flow created by the rotation of the impellers is negligible within a radius of 100 mm inside the spherical bomb. The PDFs of the normalized instantaneous field by the local RMS value have been calculated and they were found to exhibit a Gaussian shape. The skewness and flatness (kurtosis) factors were estimated to verify the validity of the Gaussian shape of the PDFs. The results are summarized in Table 1.

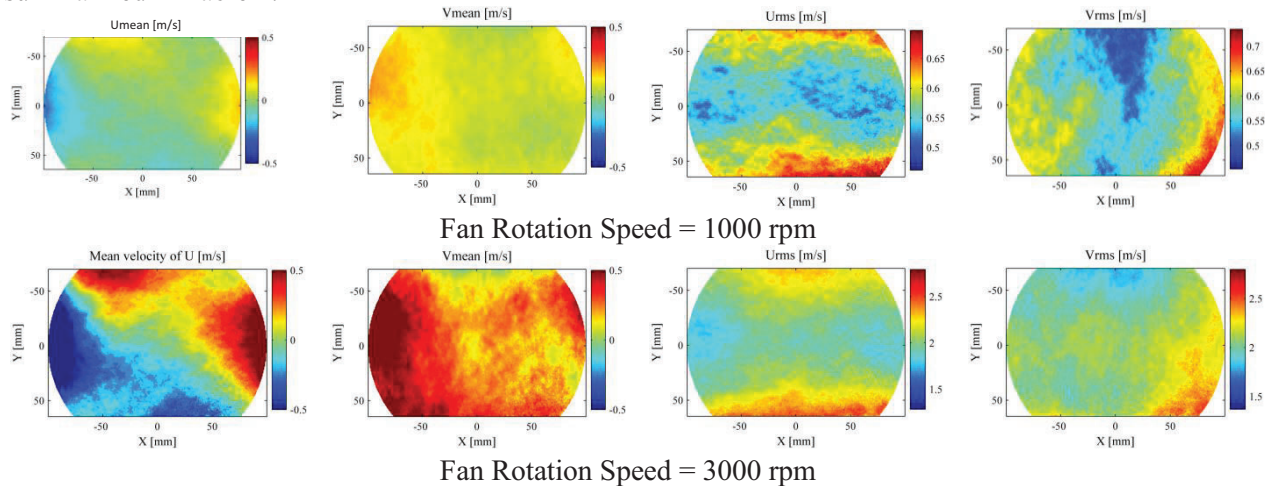


Figure 3: Maps of the velocity field obtained at two rotation speeds of the fans: average and RMS values of U and V inside the bomb.

Table I. Mean, RMS velocities and flatness and skewness factors for all rotation speeds of this study.

Rotation Speed (rpm)	$U_{mean}$ (m/s)	$V_{mean}$ (m/s)	$U_{RMS}$ (m/s)	$V_{RMS}$ (m/s)	Skewness U	Skewness V	Flatness U	Flatness V
1000	-0.01	0.09	0.56	0.57	-0.03	-0.01	3.56	3.50
2000	0.00	0.10	1.23	1.32	-0.01	-0.05	3.60	3.55
3000	-0.02	0.12	2.02	2.19	-0.01	-0.10	3.55	3.51
4000	-0.04	0.14	2.82	2.84	0.00	-0.14	3.52	3.47
5000	-0.05	0.15	3.67	3.91	0.02	-0.14	3.55	3.38

The homogeneity of the turbulence indicated to what extent the characteristics of the flowfield are independent from any local translation. It is defined as the ratio between the local RMS velocity and the spatially average one. It is plotted for both directions (x and y) in Fig. 4. The isotropy is also a desired feature which indicates that the turbulence characteristics do not change if the coordinates are rotated, they are identical in all directions. It is defined as the ratio between the RMS velocities in both directions. These two ratios tend towards the value of 1 when true. In Fig.4 then isotropy is also reported. As one can see, the homogeneity and isotropy is within 0.9-1.1 domain over a very large radius in the center of the spherical bomb.

The intensity of turbulence was found to increase linearly with the fan rotation speed as shown in Fig. 5. As for the integral length scales obtained in this study, and for the geometry of the impeller used, it was found, as expected, to be independent from the rotation speed of the fans and equal to 45 mm in the x direction and 52 mm in the y direction.

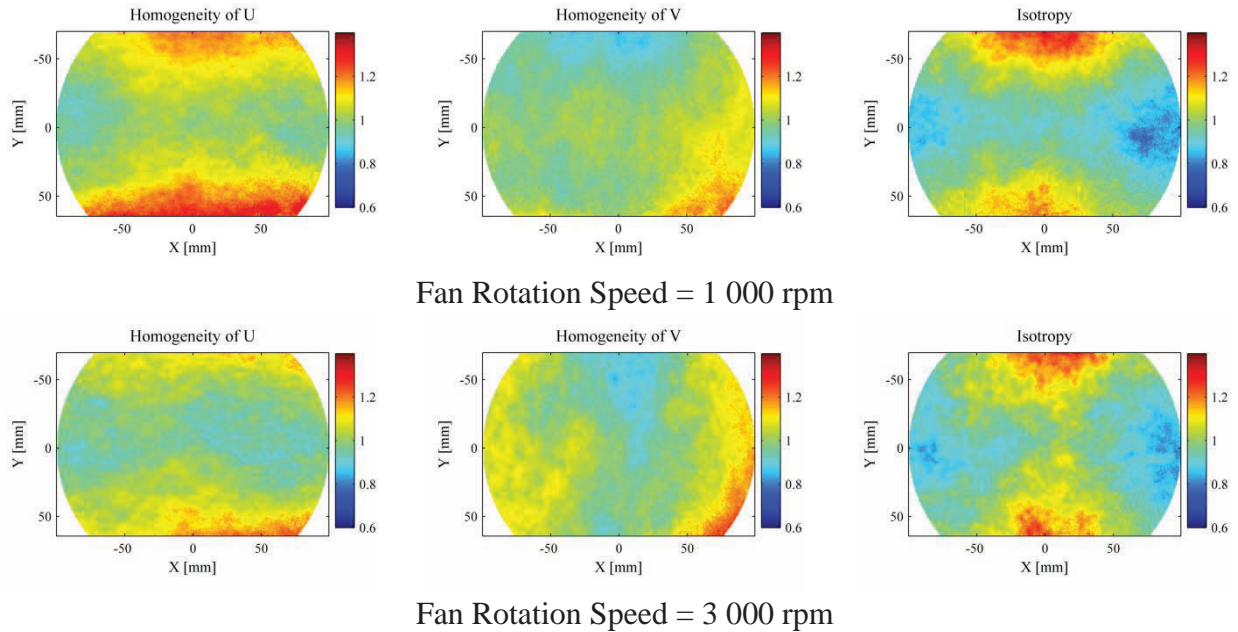


Figure 4: Homogeneity and Isotropy maps for 2 rotation speeds: 1000 and 3000 rpm.

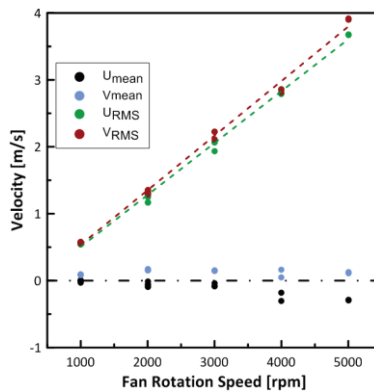


Figure 5: Evolution of the mean velocities ( $U_{\text{mean}}$ ,  $V_{\text{mean}}$ ) and of the turbulent fluctuations ( $U_{\text{RMS}}$ ,  $V_{\text{RMS}}$ ) as a function of the fan rotation speed.

### 2.3. Experimental Methodology

Before each test, the chamber was vacuumed and the residual pressure was lower than 3 Pa. The gases were introduced at the partial pressures required to give the desired mixture composition starting from  $\text{H}_2$ . The air used was dry laboratory air. Based on the precision of the pressure gauges, the concentrations were determined with an accuracy of 0.2 %. Then the fans were activated and the rotation speed set to the desired value. For the laminar experiments, the fans were not activated. Once the steady state is reached, the ignition is obtained using the spark generator and all the recording equipment are triggered on the onset of the electric spark.

The raw images, as shown in Fig. 2, are processed using an in-house code based on Matlab libraries in order to identify the edge of the flame, at each time, and determine the surface enclosed in this boundary.

From the surface of the flame, an average radius is calculated based on an equivalent circle matching the experimental area (Fig. 6). From this image processing the increase in the flame-ball size versus time can be derived and hence a turbulent displacement speed can be deduced by deriving the equivalent radius versus time. The evolution of the pressure is also recorded and can be plotted with the radius of the flame as a function of time.

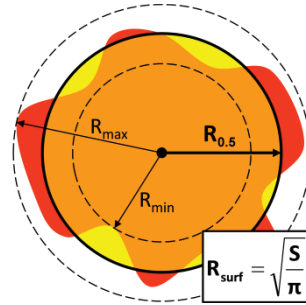


Figure 6: Definition of the flame radius based on different criteria.

The studied mixtures were constituted of H<sub>2</sub> and air and the molar fraction of H<sub>2</sub> in the mixture was varied from 0.16 to 0.28. The initial temperature and pressure were fixed at 296 K and 1 atm.

### 3. Experimental Results

The evolution of the flame radius versus time for different rotation speeds is plotted in Fig. 7 as well as the case for the laminar conditions where the fans were off. As one can see, an increase of the rotation speed, and hence the turbulent intensity associated with it, leads to an increase of the slope of the radius versus time for all the studied mixtures. On the same figure is also plotted the evolution of the pressure as a function of time. The evolution of the pressure inside the spherical vessel is also strongly affected by the presence of the initial turbulence. The total volume of the fresh gases is combusted in a much shorter time. However, the maximum overpressure reached at the end of the combustion is rigorously identical for all levels of turbulence. The experimental maximum pressure is then very close (5.7 bar and 7.76 bar at 16 % and 18 % of H<sub>2</sub> in air respectively) to the adiabatic isochoric complete combustion pressure, P<sub>AICC</sub>, of 5.97 bar at 16 % and 8.15 bar at 18 % of H<sub>2</sub> in air respectively. Similar results are obtained when the hydrogen molar percent is equal to 20 and 24 % in air. For all studied mixtures where the hydrogen molar percent was varied between 16 and 28 %, the combustion was complete independently from the level of turbulence that was achieved prior to ignition.

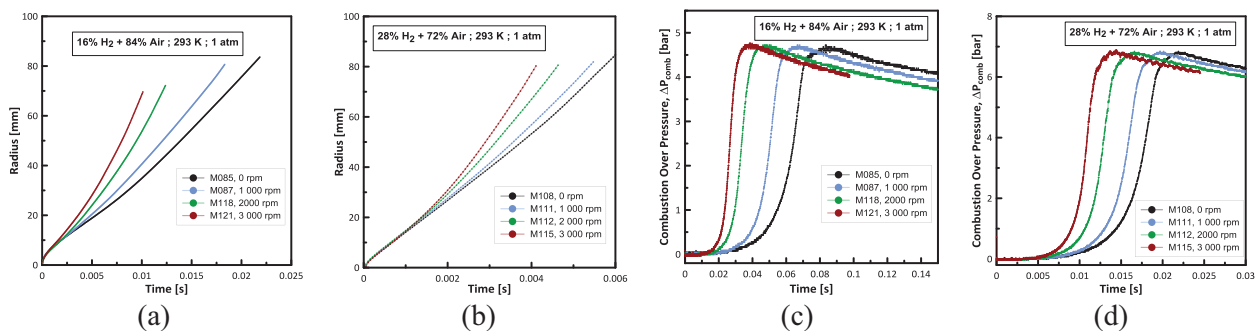


Figure 7: Evolution of the flame radius (a-b) and of the pressure (c-d) during the combustion of H<sub>2</sub> / air mixtures initially at 1 atm and 293 K for different fan rotation speeds as well as the quiescent case).

The turbulent flame velocity is derived from the evolution of the flame radius versus time. The reader has to keep in mind that there is no consensus on the definition of the turbulent flame speed when comparing different flame configurations [3, 4]: a turbulent flame measured in a burner configuration is generally defined based on a progress variable corresponding to a consumption speed of 50 % of the unburnt gases while for an expanding spherical flame the definition of the turbulent speed is based on the outer edge of a Schlieren image of the flame. Since the flame surface is wrinkled, either due to the turbulence in the medium, or due to the thermo-diffusive instabilities in the case of lean hydrogen/air mixtures, an average radius is derived based on an equivalent flame area as defined in Fig. 6. In this study the burning speed is evaluated on this latter definition:

$$S_b = \frac{dR_{\text{Surf}}}{dt} \quad (1)$$

When the mixture is at rest, the derived burning speed correspond to the laminar burning speed,  $S_{b,L}$  and when the fans are activated at a given rotation speed, the derived burning speed corresponds to the turbulent burning speed,  $S_{b,t}$ . A central difference is used to derive the flame speed from the radius as a function of time. Fig. 8 shows the evolution of the flame speed with and without turbulence in the vessel.

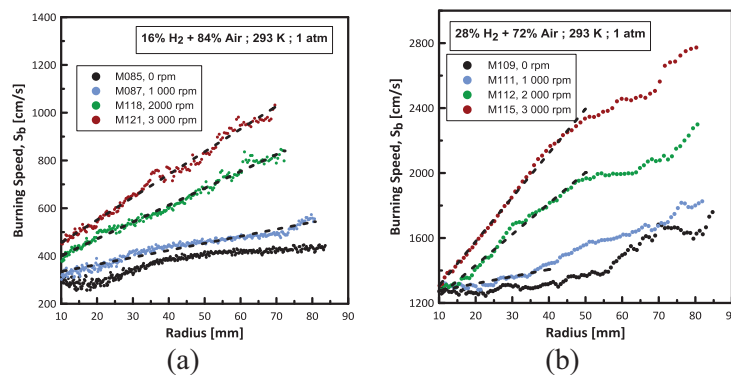


Figure 8: Evolution of the burning speed as a function of the flame radius during the combustion of H<sub>2</sub> / air mixtures initially at 1 atm and 293 K for different fan rotation speeds as well as the quiescent case.

In the case where no turbulence was created prior to the ignition of the flame, the behavior of the flame speed as the radius of the flame increases depends strongly on the hydrogen molar percent:

- For the mixture containing 16 % of hydrogen in air, the laminar burning speed,  $S_{b,L}$ , increases with the radius of the flame up to a radius of around 40 mm, then remains constant as the radius increases further;
- In the case where the mixture contains 28 % of hydrogen, the flame propagates at almost constant laminar burning speed until it reaches a radius of about 40 mm and then undergoes an acceleration that is strongly marked at a radius of around 60 mm. This sudden increase in the velocity is directly linked to the onset of instabilities that wrinkles the flame and induces this increase.

In case where turbulence is created in the vessel prior the ignition of the mixture, we observe that the burning speed is increased with the initial turbulent intensity at all flame radii. However, this increase, for a given turbulent intensity, depends on the initial hydrogen content of the mixture:

- when the mixture contains 16 % of hydrogen, the turbulent burning speed increases linearly with the flame radius at all turbulent fluctuations;
- when the mixture contains 28 % of hydrogen in air, the turbulent burning speed varies linearly as the flame radius is increased up to a critical radius that depends on the turbulent fluctuation. This critical radius is around 35 mm when the turbulent fluctuation is around 0.56 m/s (1000 rpm) and is around

50 mm when the turbulent fluctuation is equal to 3.79 m/s (5000 rpm). Beyond this critical radius, the burning speed increase levels-off for a certain distance before increasing again.

In order to analyze further the data, it is important to know the laminar flame speed and the laminar flame thickness of hydrogen / air mixtures at the experimental conditions. The laminar flame speeds have been determined using the spherical method and used to choose the best detailed kinetic mechanism in order to determine the flame speeds for mixtures where the experimental determination is not feasible. Indeed, for very lean mixtures, the thermo-diffusive instabilities will be responsible for an early wrinkling of the flame which will prevent from deriving a proper laminar flame speed. Fig. 9 summarizes the results of this study in terms of variation of the laminar flame speed with the equivalence ratio (a), Markstein lengths (b), based on unburned and burnt gases and flame thickness (c) based on the maximum gradient of the temperature or on the thermal diffusivity.

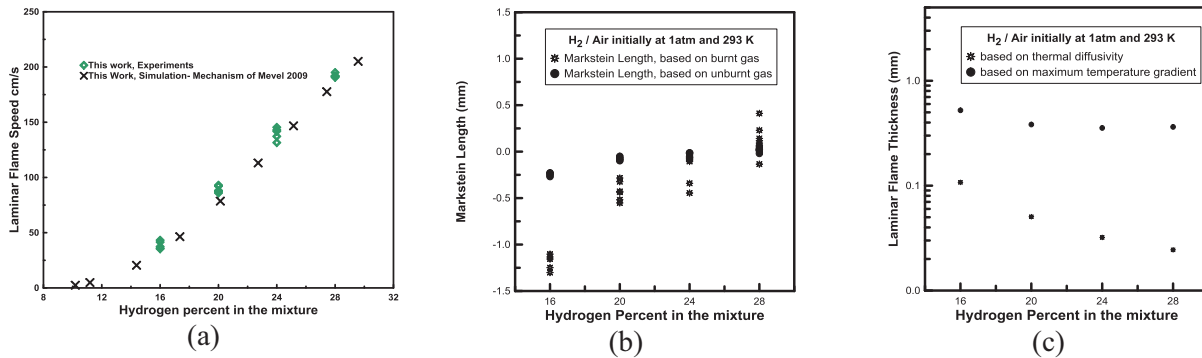


Figure 9: Laminar flame speed (a), Markstein length (b) and flame thickness (c) as a function of the equivalence ratio of H<sub>2</sub> / air mixtures initially at 1 atm and 300 K.

Using the data plotted in Fig. 9 allows the identification of the experiments conducted in this study in the Borghi diagram where the different turbulent regimes are identified by plotting the normalized turbulent intensity versus the normalized integral length scale as plotted in Fig. 10. Most of the present study conditions cover the domain from wrinkled laminar flames to the “thickened regime”. All experiments are below the Damköhler number equal to 1 which indicates that, to a certain extent, the flamelet structure is maintained. As the analysis performed in [8] shows that the turbulent integral scale in reactor containment is between 0.02 and 2 m and the velocity RMS is between 0.03 and 15 m/s, the combustion regime expected in reactor containment is flamelet regime. Thus, the investigated domain cover the situation expected in nuclear reactor containment in severe accident conditions

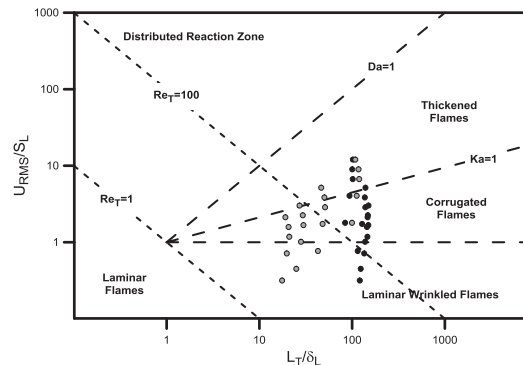


Figure 10: Turbulent combustion diagram with the conditions of the present study as closed symbols.

In order to analyze the experimental results, the turbulent speed,  $S_{b,t}$  is normalized by the unstretched burning speed  $S_b^0$  and the flame radius by the turbulent length scale,  $L_T$ . As one can see in Fig. 11, the normalized turbulent flame speed varies strongly with the normalized flame size. For the mixture containing 16% of  $H_2$  in air, the increase is almost linear, while the mixture containing 28% of  $H_2$  exhibits a non-linear increase.

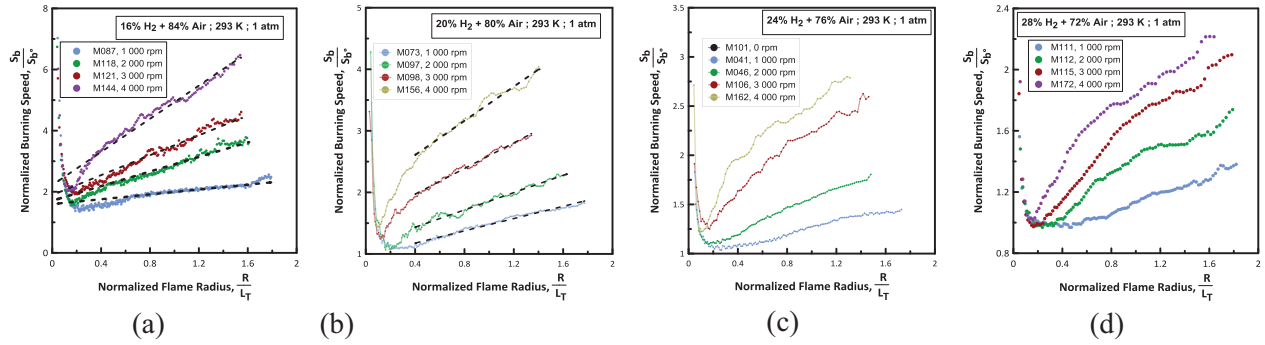


Figure 11: Evolution of the normalized turbulent flame speed versus the normalized flame radius.

In Fig. 12, the evolution of the normalized turbulent flame speed is plotted versus the normalized turbulence intensity (equal to the RMS of the velocity fluctuation as specified in table I) by the unstretched laminar flame speed (a to d) and as a function of the normalized flame radius (e to h).

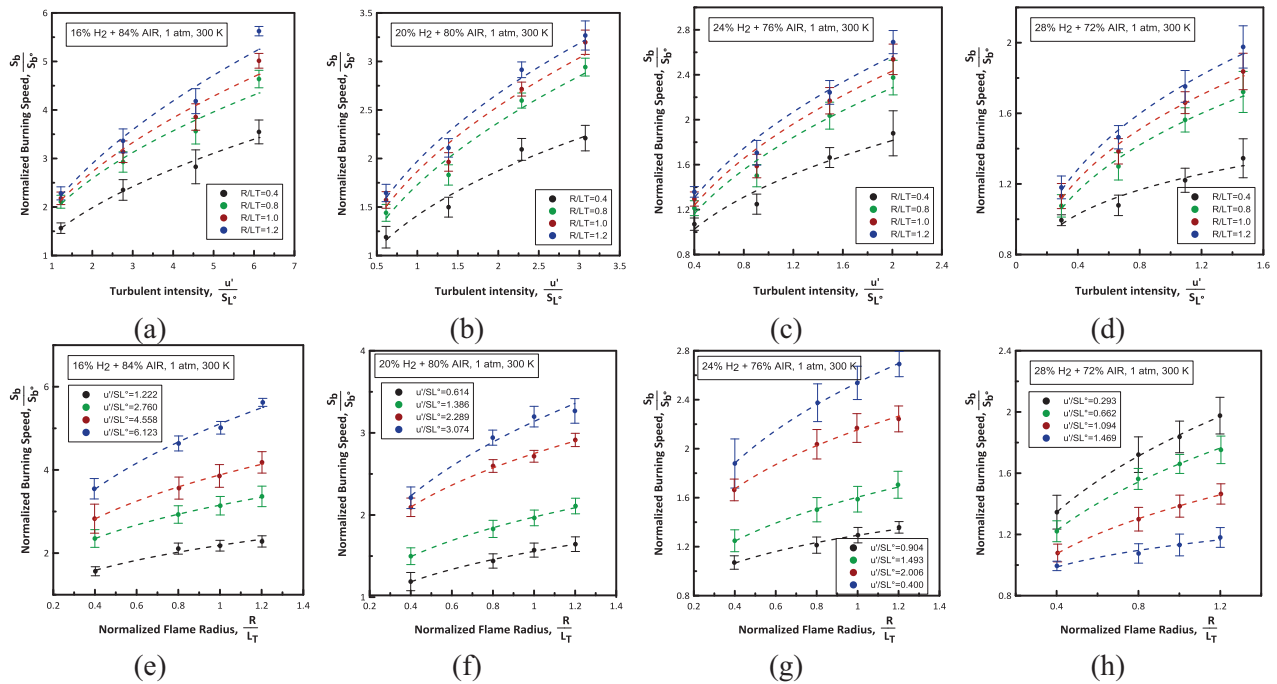


Figure 12: Evolution of the normalized turbulent flame speed versus the turbulent intensity.

This figure shows that the normalized turbulent flame speed varies according to the following expression:

$$\frac{S_{b,t}}{S_b^0} \approx \left( \frac{u'}{S_L^0} \right)^\alpha \cdot \left( \frac{R}{L_T} \right)^\beta \quad (2)$$

Using a multiple regression, the coefficients  $\alpha$  and  $\beta$  were found to be equal to  $0.471 \pm 0.015$  and  $0.306 \pm 0.030$  respectively with an  $R^2 = 0.94$ . The  $\alpha$  coefficient derived in this study is in agreement with the literature [5,6]. However, for the coefficient  $\beta$ , there were no data in the literature to compare with for lean mixtures of hydrogen in air, in the case of spherical expanding flames. Most of the recent studies focus on stable mixtures with positive Markstein lengths [7].

#### 4. CONCLUSIONS

This study presented new results obtained in a new facility designed and built at our laboratory, CNRS-ICARE. The setup consists of a spherical bomb equipped with 8 fans that are mounted symmetrically along the inner wall of the bomb. It was demonstrated we were able to produce a large volume (around 100 mm in radius) inside the spherical vessel where the turbulence is indeed homogeneous and isotropic with intensities that varies from 0.57 m/s up to 3.79 m/s. With this new facility, the turbulent flame speed of lean mixtures of hydrogen / air mixtures with hydrogen molar percent between 16 and 28 % were determined. A correlation between turbulent speed and turbulent integral scale is proposed and will be used to improve safety analyses of CFD codes predictions.

#### ACKNOWLEDGMENTS

The authors acknowledge the financial support of the IRSN.

#### REFERENCES

1. A. Bentaib, A. Bleyer, N. Meynet, N. Chaumeix, B. Schramm, M. Höhne, P. Kostka, M. Movahed, S. Worapittayaporn, T. Brähler, H. Seok-Kang, M. Povilaitis, I. Kljenak, P. Sathiah, "SARNET hydrogen deflagration benchmarks: Main outcomes and conclusions", *Annals of Nuclear Energy*, **74**, pp. 143-152 (2014)
2. OECD NEA report, "ISP-49 on Hydrogen Combustion", CSNI/R(2011)9, January 2012
3. D. Bradley, M. Lawes, M. S. Mansour, "Correlation of Turbulent Burning Velocities of Ethanol-Air, Measured in a Fan-Stirred Bomb up to 1.2 MPa", *Combust. Flame*, **158**, pp. 123-138 (2011).
4. C. Mandilas, M.P. Ormsby, C.G.W. Sheppard, R. Woolley, "Effects of hydrogen addition on laminar and turbulent premixed methane and iso-octane-air flames", *Proceedings of the Combustion Institute*, **31**(1), pp. 1443-1450 (2007)
5. D. Bradley, A. C. K. Law, and M. Lawes. "Flame stretch rate as a determinant of turbulent burning velocity", *Phil. Trans. Roy. Soc. London*, **A338**, pp. 359-387 (1992).
6. N. Peters. "The turbulent burning velocity for large-scale and small-scale turbulence". *Journal of Fluid Mechanics*, **384**, pp. 107-132 (1999).
7. F. Wu, A. Saha, S.o Chaudhuri, C. K. Law, "Propagation speeds of expanding turbulent flames of C4 to C8 n-alkanes at elevated pressures: Experimental determination, fuel similarity, and stretch-affected local extinction", *Proceedings of the Combustion Institute*, **35** (2), pp. 1501-1508 (2015)
8. A. Faix, "Phénoménologie et calculs numériques de la propagation d'une flamme de prémélange hydrogène-air pauvre dans un milieu turbulent", Ph.D. Thesis. Université d'Orléans 2005